

# Fourling Operations on $\text{ReO}_3$ -Related Structures. Intergrowths and Defects

Bengt-Olov Marinder

Department of Inorganic Chemistry, Arrhenius Laboratory, Stockholm University, S-106 91 Stockholm, Sweden

Marinder, B.-O., 1991. Fourling Operations on  $\text{ReO}_3$ -Related Structures. Intergrowths and Defects. – Acta Chem. Scand. 45: 659–668.

Structures of composition  $A_yMX_3$  (I),  $A_yMX_{3-z}$  (II) and  $A_yMX_{3+z}$  (III) are described by means of fourling units derived from parent structures of  $\text{ReO}_3$  or similar types.  $A$  represents cations inserted into tunnels of the network structure;  $z > 0$ ,  $y \geq 0$ . Type I includes tungsten bronzes (HTB and ITB),  $\text{Ca}_2\text{TlTa}_5\text{O}_{15}$ ,  $\text{Ba}_4\text{FeTa}_{10}\text{O}_{30}$  and tilted  $\text{ReO}_3(t)$ . Type II is represented by  $\text{NaNb}_6\text{O}_{15}\text{F}$ ,  $\beta\text{-U}_3\text{O}_8$ ,  $\text{UMo}_2\text{O}_8$ ; type III by  $\text{KIn}_2\text{F}_7$ ,  $\text{U}_2\text{O}_2\text{Cl}_5$ ,  $\text{RbIn}_3\text{F}_{10}$ ,  $\text{Rb}_2\text{In}_3\text{F}_{11}$  and  $\text{Cs}_{1-x}\text{Lu}_3\text{F}_{10-x}$ . Several of these structures are able to form intergrowths with each other. The relationship between local twin planes (in a saw-tooth or meander form) and fourling units of tetragonal symmetry is discussed. Fourling units are also used to describe defects as observed by high-resolution electron microscopy (HREM) in oxides of HTB and ITB types.

The idea of chemical twinning on the unit-cell level was introduced by Andersson and Hyde in 1974 as a means to describe several complicated structures.<sup>1</sup> They found that many structures can be perceived as arrangements of atoms (in most cases close-packed arrays) on which a repeated twin operation is carried out. The original atomic arrangement is called a parent structure. The twin operation on the parent structure gives rise to twin units related to each other by a reflection or a rotation.<sup>2,3</sup> If this operation is a reflection, the plane on which the twin units are joined (the composition plane) is a mirror (or twin) plane. In the mirror plane additional atoms may be inserted. Thus the olivine-type structure ( $\text{Mg}_2\text{SiO}_4$ ) can be thought of as built up by regularly repeated twinning on  $\{031\}$  of a rutile-type structure with silicon atoms in tetrahedral coordination within the twin planes.<sup>4</sup>

In the structure of cementite,  $\text{Fe}_3\text{C}$ , a hexagonally close-packed arrangement of iron atoms is regularly twinned on  $(11\bar{2}2)_{\text{hex}}$ . In the planes, the iron atoms form trigonal prisms which house the carbon atoms. In this case the twin operation provides the structure with another and larger type of interstice than that available in the parent structure, which facilitates the accommodation of the carbon atoms.

Repeated twinning of an  $\text{ReO}_3$ -type structure on  $(2\bar{1}0)$  gives rise to the  $\text{LiNb}_6\text{O}_{15}\text{F}$  and  $\text{NaNb}_6\text{O}_{15}\text{F}$  structures.<sup>5</sup> As a result of the twinning operation, trigonal prisms of oxygen atoms are created in the twin planes. These prisms may accommodate larger cations such as sodium in  $\text{NaNb}_6\text{O}_{15}\text{F}$ . The twin planes also exhibit planar pentagons of oxygen atoms. In  $\text{LiNb}_6\text{O}_{15}\text{F}$  and  $\text{NaNb}_6\text{O}_{15}\text{F}$ , strings of  $\text{Nb-O-Nb-O-}$  may be inserted in the twin planes, with a metal atom at the centre of a pentagon and with the string perpendicular to the plane. In this way pentagonal bipyramids are created in the twin plane. The whole assembly of a

pentagonal bipyramid and the surrounding five octahedra is called a pentagonal column (PC).<sup>6</sup>

A parent structure of the  $R\text{-Nb}_2\text{O}_5$  type twinned on  $(0\bar{1}1)$  gives rise to several structures related to the high-pressure modification of  $\text{Nb}_3\text{O}_7\text{F}$ .<sup>7</sup> An alternative parent structure is  $\text{ReO}_3$  with antiphase boundaries (APBs). Here the twinning takes place on  $(3\bar{1}0)$  of  $\text{ReO}_3$ . This type of twinning may create pentagonal bipyramids but not PCs.

Twinning as a structure-building operation is variously termed unit-cell twinning, chemical twinning or non-conservative twinning. Unit-cell twinning implies that the unit cell of the parent structure is a subcell of the resulting structure.<sup>8</sup> (Originally it was stated<sup>1</sup> that the periodicity of the twin planes determines the size of the unit cell of the resulting structure.) Thus the olivine structure is described as a unit-cell twinned rutile type, with additional, tetrahedral cations in the composition planes.<sup>4</sup>

The term 'chemical twinning' is used by analogy with the relief of mechanical stress by mechanical twinning.<sup>8</sup> The chemical stress relieved is the need for larger interstices for some atoms (e.g. the carbon atoms in  $\text{Fe}_3\text{C}$ ) which are accommodated in the trigonal prisms of twin planes. As regards the twin operation in  $\text{LiNb}_6\text{O}_{15}\text{F}$  and in similar, PC-containing compounds, the PCs seem to form as a response to the actual stoichiometry, i.e. when the ratio of anions to (higher-valent) cations in the reactants is below some critical value.

Van Landuyt *et al.*<sup>9</sup> found in a study of hexagonal ferrites of the  $\text{BaFe}_{12}\text{O}_{19}$  type that their structural complexity could be simplified by considering the structures as periodic twins. The twinning is accompanied by a change in composition (in this case a small deficiency of Ba atoms). It is therefore called 'nonconservative twinning'. These authors also suggest that during the growth of the crystals, from a

flux of a given composition, they may be induced to twin when the concentration of Ba atoms in the flux near the crystal happens to be somewhat below the average value; i.e. the occurrence of twins is stoichiometry-dependent. The situation is more complex, however, as a crystallographic shear plane may also be introduced into the crystal, causing an excess of Ba atoms to be accommodated.

We will use the terms unit-cell twinning and chemical twinning interchangeably when referring to twinning as a structure-building operation.

The structures mentioned above can all be described by parallel reflection operations. Thus the derived structures exhibit *one* set of parallel twin or mirror planes. In this paper we will describe some structures of oxides, fluorides and oxide halogenides that contain *two* sets of twin planes, perpendicular to each other and circumscribing a so-called fourling unit<sup>10</sup> of a parent structure. The parent structures (ideal or somewhat deformed) are either of the  $\text{ReO}_3$  type or derived from it [ $\text{ReO}_3$  with antiphase boundaries (APBs) or  $R\text{-Nb}_2\text{O}_5$ ].

#### Fourling operations on $\text{ReO}_3$

Figs. 1(a)–(c) show three hypothetical structures derived from undistorted  $\text{ReO}_3$ , as shown on the left where the two sets of twin planes are also indicated. Models of the fourling units are shown separately, and their proportions are indicated in the figure by a scale where one unit is  $a/\sqrt{5}$ ,  $a$  being the length of an edge of a regular octahedron. Note that, when a twin plane penetrates an octahedron, the

$M\text{-O-M-O}$ -string perpendicular to the plane of projection has to move slightly so as to coincide with the twin plane.

The structure shown in Fig. 1(b) can alternatively be described as originating from the rotation of rows of octahedra in an  $\text{ReO}_3$ -type structure. The tilt (or rotation), through an angle of  $15^\circ$ , is on an axis perpendicular to the plane of the paper. The tilt axis is parallel with one of the cube axes of  $\text{ReO}_3$  (a one-tilt system according to Glazer,<sup>11</sup> who considers tilting of octahedra in perovskites). The tilting of one row of octahedra causes neighbouring rows to rotate in the opposite direction. The tilt makes the resulting structure more compact than  $\text{ReO}_3$ , since the O atoms in the equatorial plane increase their anion coordination from 8 to 9 and the cell volume is decreased by 6.7%.<sup>12</sup> No compound seems to have adopted this structure, sometimes referred to as completely collapsed  $\text{ReO}_3$ ,<sup>13</sup> but it is an integral part of, e.g., intergrowth tungsten bronzes<sup>12</sup> (see below). In the following we will refer to this structure type with tilted octahedra as  $\text{ReO}_3(\text{t})$ .

The other two structures [Figs. 1(a) and (c)] both contain pentagonal bipyramids and have an  $\text{MX}_{3.5}$  stoichiometry. The one of tetragonal symmetry, Fig. 1(c), has been proposed as a possible structure for an end member of a series  $\text{MX}_{4-x}$ , with  $x = 0.5$ , in the system  $\text{ZrO}_2\text{-ZrF}_4$ .<sup>14</sup> It is also given as the crystal structure of a zirconium oxide hydroxide fluoride with  $\text{ZrX}_{3.5}$  stoichiometry.<sup>10</sup> Note that by use of the fourling unit indicated in the lower right part of the structure in Fig. 1(c) we may obtain, by a four-fold rotation, the structure shown in Fig. 1(d). It has the composition  $(\text{MX})_4\text{X}'$ , ( $\text{X}'$  denoting the equatorial anions in the

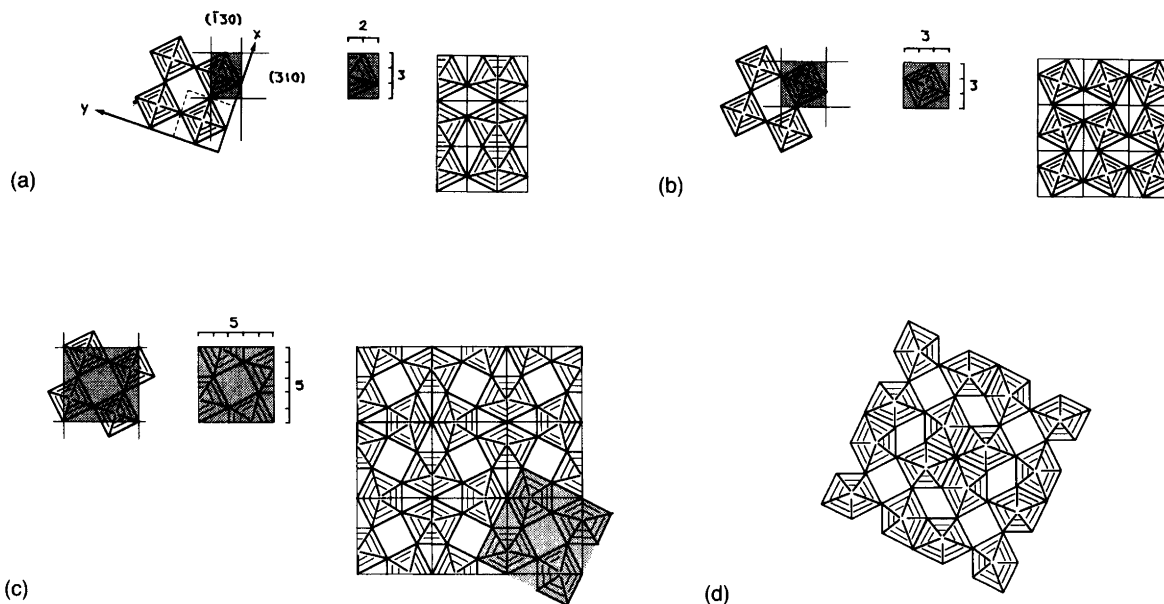


Fig. 1. To the right are hypothetical structures shown in projection and derived from undistorted  $\text{ReO}_3$ , shown to the left. The fourling units in this and later figures are shown in the middle, and their proportions are indicated by a scale next to the figures. In the left figures two sets of twin planes are shown, with orientations  $(130)$  and  $(310)$ . A unit cell of  $\text{ReO}_3$  is indicated in (a). (a)  $\text{M}_2\text{X}_7$  (orthorhombic); (b)  $\text{MX}_3$  of the tilted  $\text{ReO}_3$  type; (c)  $\text{M}_2\text{X}_7$  (tetragonal); (d) a tetragonal structure with  $\text{M}_4\text{X}_{13}$  composition, derived through a four-fold rotation of a fourling unit obtained from the structure in (c).

pentagonal bipyramids). The  $X'$  net has been discussed by O'Keeffe and Hyde.<sup>15</sup>

There is an interesting relationship between the structure in Fig. 1(c) and that of  $Ba_3In_2F_{12}$ .<sup>16</sup> For the sake of comparison we will consider the anions of the structure in Fig. 1(c). They form two nets,  $A$  and  $B$ .  $A$  is composed of the equatorial ions of the bipyramids, while  $B$  is made up of the top (or bottom) ions. The anion structure can now be described as an arrangement  $ABAB\dots$  along the tetragonal axis. The fluorine structure of  $Ba_3In_2F_{12}$  is also built up of the same  $A$  and  $B$  nets but in a different stacking along the tetragonal axis:  $ABBAAB\dots$ . Two Ba atoms are eight-coordinated in the four-sided tunnels, while four Ba atoms are 12-coordinated at the centre of a pentagonal prism, bi-capped at top and bottom. Four In atoms are in mono-capped trigonal prisms.

The other derived structure (of orthorhombic symmetry) Fig. 1(a) is, it seems, only a hypothetical structure. It will be discussed further below.

The derivation of the following structures from the  $ReO_3$  type presupposes a deformation of the parent structure as

shown in Figs. 2(a)–(e). The two sets of planes parallel with  $(\bar{1}20)$  and  $(210)$  in  $ReO_3$  have turned into planes parallel with  $(\bar{1}30)$  and  $(310)$  in the fourling units. The orientation of the twin planes is then the same as the one shown by the twin planes in Figs. 1(a)–(c).

The deformation of the parent structure has as a consequence the occurrence of two differently sized octahedra in some of the models. The lengths of the equatorial edges of the two types are  $a$  and  $2a/\sqrt{5}$ . The advantage of this model is the ease with which one can draw the structures on a piece of graph paper using the scale shown next to the fourling units.

Fig. 2(a) shows the crystal structure of  $RbIn_3F_{10}$ .<sup>17</sup> One third of the indium atoms are six-coordinated (octahedra) and two thirds are seven-coordinated (pentagonal bipyramids). The Rb atoms are located in the tunnels.

Fig. 2(b) shows the crystal structure of  $Ca_2TiTa_5O_{15}$ <sup>18</sup> (and the isostructural  $Ca_2RbTa_5O_{15}$  and  $Ca_2CsTa_5O_{15}$ ). The tantalum atoms are six-coordinated (octahedra) while the thallium atoms are statistically distributed near the centre of the cavities limited by  $(12+6)$  oxygen atoms. The

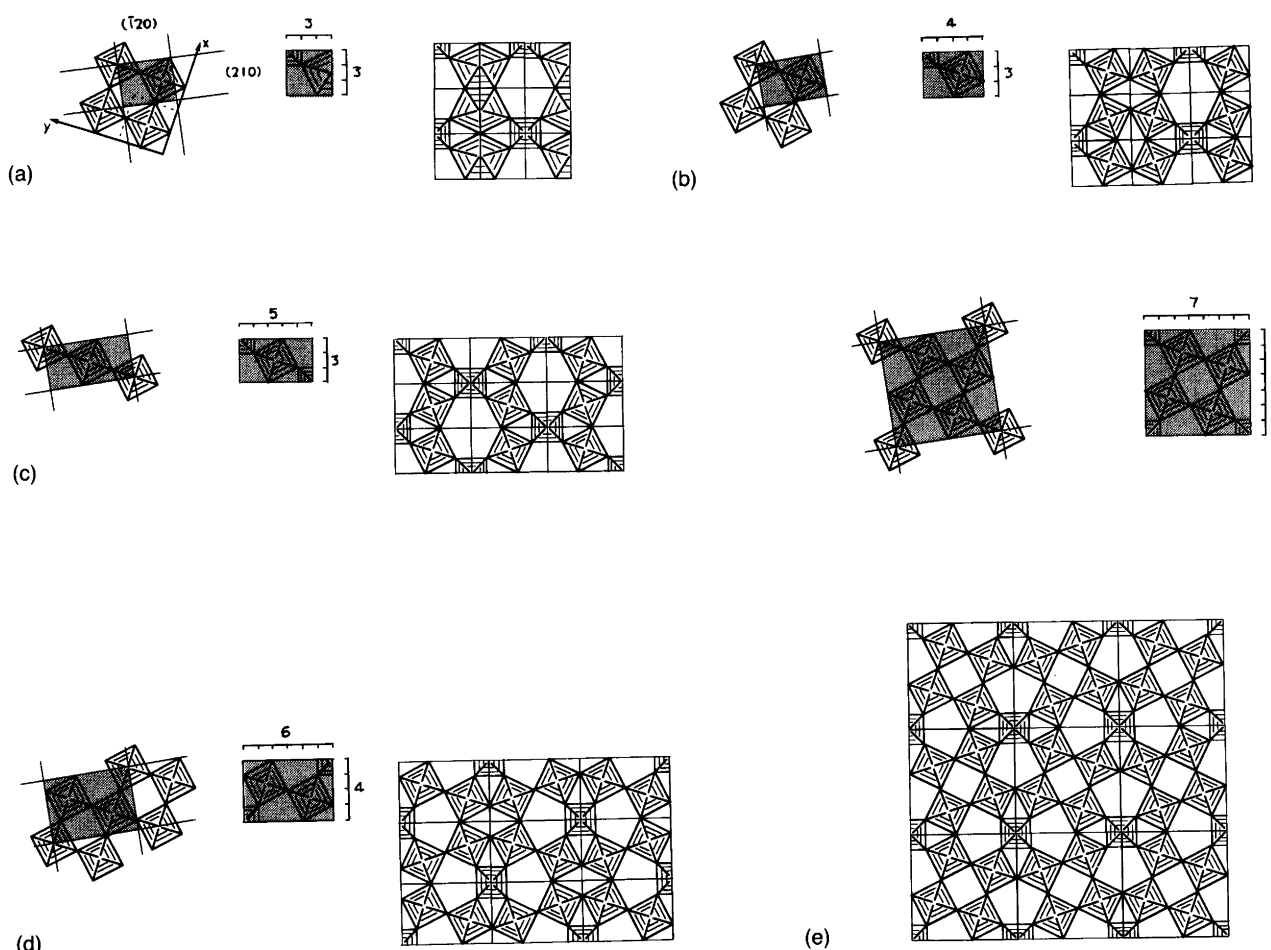


Fig. 2. Crystal structures derived from distorted  $ReO_3$  are shown to the right. Two sets of planes, with orientations  $(\bar{1}20)$  and  $(210)$  as referred to the unit cell of  $ReO_3$  in (a), are shown to the left. The fourling units in the middle have their twin planes oriented parallel with  $(\bar{1}30)$  and  $(310)$  as in Figs. 1(a)–(c). Only the skeleton networks are given. (a)  $RbIn_3F_{10}$ ;<sup>17</sup> (b)  $Ca_2TiTa_5O_{15}$ ;<sup>18</sup> (c) hexagonal tungsten bronze, HTB;<sup>19</sup> (d)  $Ba_4FeTa_{10}O_{30}$ ;<sup>20</sup> (e) tetragonal tungsten bronze, TTB.<sup>23</sup>

calcium atoms are statistically distributed in the cavities formed by the four strings of octahedra running perpendicular to the plane of the projection.

Fig. 2(c) shows a closely related structure, namely that of hexagonal tungsten bronze (HTB).<sup>19</sup> The  $\text{WO}_6$  octahedra form three- and six-membered rings by corner sharing. The large alkali-metal atoms are distributed in the cavities limited by  $(12 + 6)$  oxygen atoms.

Fig. 2(d) shows how the crystal structure of  $\text{Ba}_4\text{FeTa}_{10}\text{O}_{30}$ <sup>20</sup> is derived from the  $\text{ReO}_3$  type. The Ba atoms occupy the five-sided tunnels, and Fe atoms partly occupy the cavities formed by the octahedra. The structures of  $\text{NaNb}_6\text{O}_{15}\text{F}$ <sup>21</sup> and  $\text{SrNb}_6\text{O}_{16}$ <sup>22</sup> are quite similar ( $\text{NaNb}_6\text{O}_{15}\text{F}$  has earlier<sup>5</sup> been described using *one* set of twin planes). Two of the Ba sites are occupied by Nb-X-Nb-X- strings forming PCs. Thus only the skeleton networks in these two structures are built of fourling units.

Fig. 2(e) finally shows the skeleton net of tetragonal tungsten bronze (TTB).<sup>23</sup> This structure has earlier been described as derived by a chemical fourling operation on  $\text{ReO}_3$ <sup>10</sup> or by a rotation operation on  $\text{ReO}_3$  rows,  $2 \times 2$  octahedra in cross-section.<sup>24</sup> This structure type will be discussed further below.

#### Fourling operations on $\text{ReO}_3$ with APBs

Fig. 3(a) shows how the crystal structure of  $\text{Rb}_2\text{In}_3\text{F}_{11}$  is derived from a deformed structure of the  $\text{ReO}_3$  type with APBs.<sup>25</sup> The parent structure is the skeleton net found in

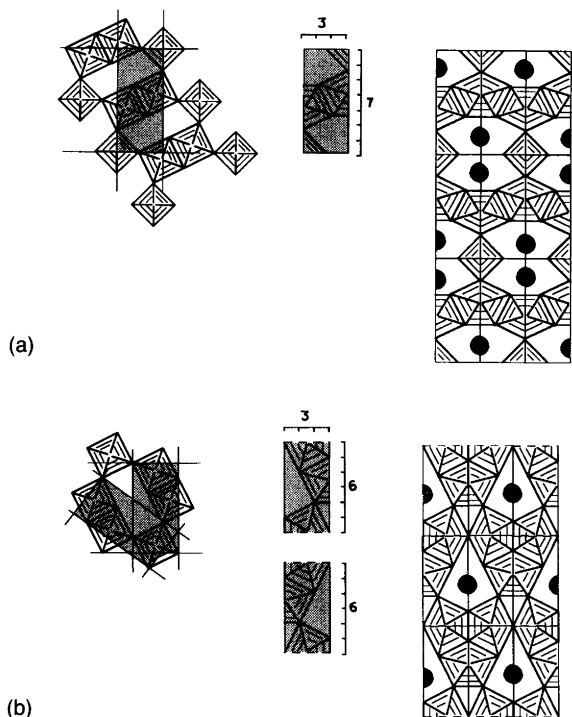


Fig. 3. Crystal structures derived from antiphase boundaries in  $\text{ReO}_3$ . Filled circles indicate alkali-metal atoms. (a)  $\text{Rb}_2\text{In}_3\text{F}_{11}$ ,<sup>25</sup> (b)  $\text{Cs}_{1-x}\text{Lu}_3\text{F}_{10-x}$ .<sup>27</sup>

the low-temperature form of  $\text{LaNb}_3\text{O}_9$ ,<sup>26</sup> where the  $\text{NbO}_6$  octahedra are so arranged. Rubidium atoms reside in the tunnels.

The ideal structure of  $\text{Cs}_{1-x}\text{Lu}_3\text{F}_{10-x}$ <sup>27</sup> is shown in Fig. 3(b). It may be thought of as built up by repeated parallel twinning of a module composed of two parts taken from  $\text{ReO}_3$ , with APBs as shown in the figure. The parts are circumscribed by one set of ordinary twin planes and one set of pseudo-twin planes, which cause the parts to fit together to form the module. Thus the structure is not a true fourling structure, but we include it here since we wish to compare it with  $\text{ReO}_3(t)$  and other true fourling structures.

The structure of  $\beta\text{-U}_3\text{O}_8$  has previously been derived from  $\text{ReO}_3$  with APBs.<sup>28</sup> It can, however, be better described as derived from  $R\text{-Nb}_2\text{O}_5$ , as will be shown below.

#### Fourling operations on $R\text{-Nb}_2\text{O}_5$

Part of the structure of  $R\text{-Nb}_2\text{O}_5$ <sup>29</sup> is shown to the left in Fig. 4(a). It is derived from  $\text{ReO}_3$  through repeated crystallographic shear parallel to (001). The crystal struc-

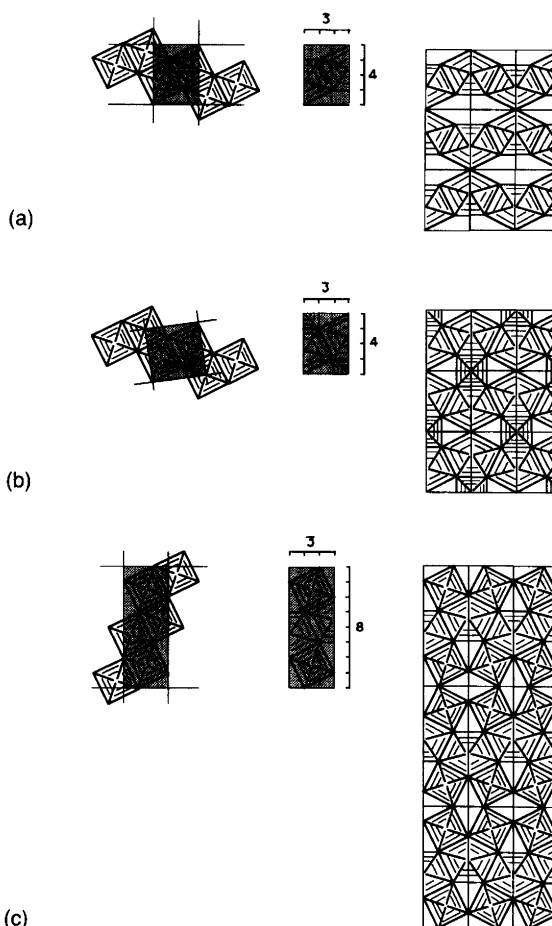
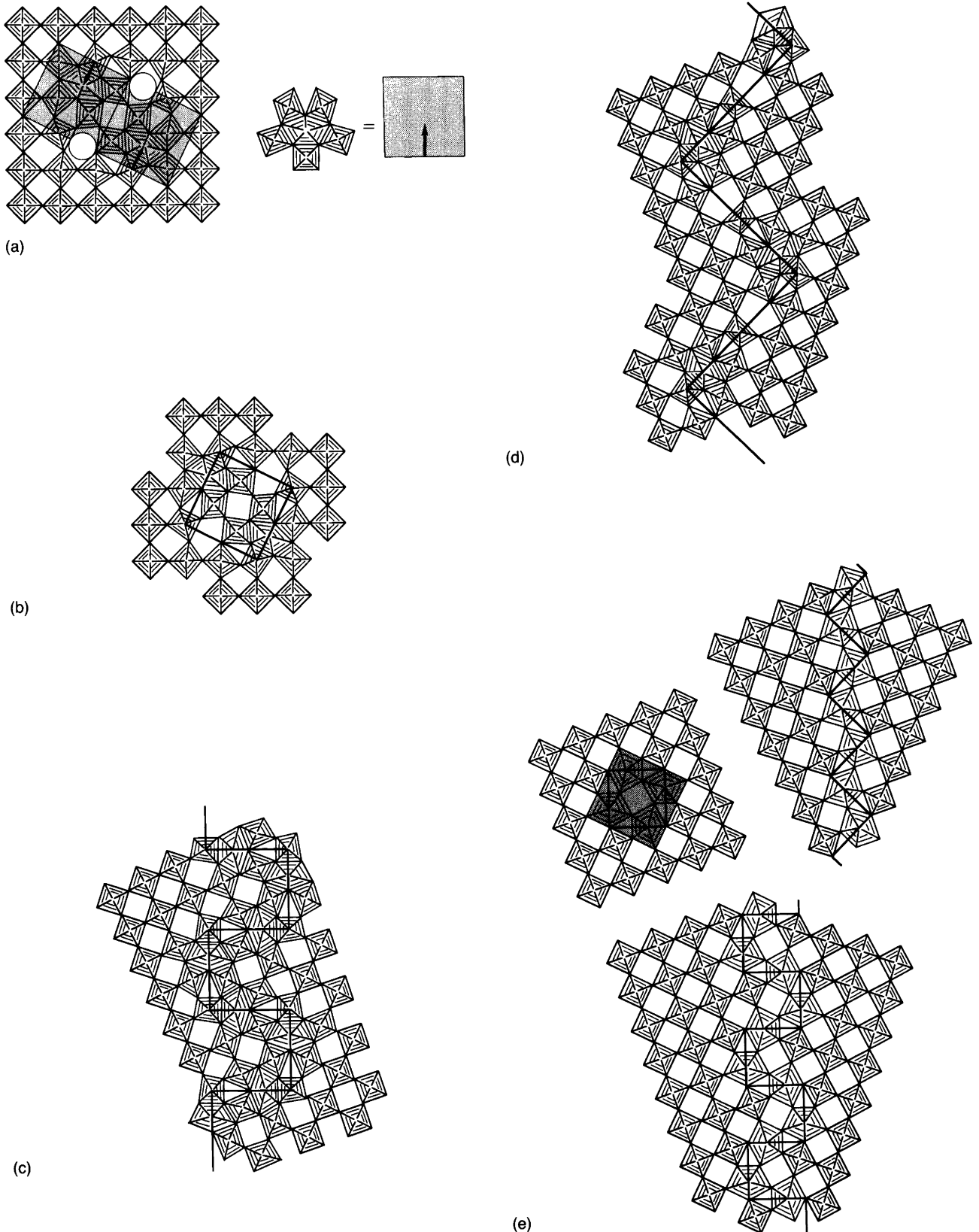


Fig. 4. Crystal structures derived from  $R\text{-Nb}_2\text{O}_5$  as shown to the left. (a)  $\text{U}_2\text{O}_2\text{Cl}_5$ <sup>30</sup> and  $\text{KIn}_2\text{F}_7$ ,<sup>31</sup> note that the tunnels are empty in  $\text{U}_2\text{O}_2\text{Cl}_5$  and filled by K atoms in  $\text{KIn}_2\text{F}_7$ ; (b)  $\text{Nb}_3\text{O}_7\text{F}(\text{hp})$ <sup>33</sup> and  $\beta\text{-U}_3\text{O}_8$ ,<sup>7,28,32</sup> (c)  $\text{UMo}_2\text{O}_8$ .<sup>34</sup>



*Fig. 5.* (a) Two pentagonal columns (PCs) embedded in an ReO<sub>3</sub>-type matrix. A shorthand notation for a PC is also shown. (b) As (a) but the presence of local twin planes is shown in bold outline. (c) Local twin planes in meander form and (d) in saw-tooth form, as observed in reorientation boundaries in the WO<sub>3</sub>-rich part of the Nb<sub>2</sub>O<sub>5</sub>-WO<sub>3</sub> system.<sup>36</sup> (e) Local twin planes with pentagonal bipyramids in an ReO<sub>3</sub>-type matrix. Note the shadowed unit of Fig. 1(c) in the left-hand figure.

ture of  $U_2O_2Cl_5$ <sup>30</sup> and  $KIn_2F_7$ <sup>31</sup> is shown to the right. The tunnels are empty in  $U_2O_2Cl_5$  but host the alkali-metal atoms in  $KIn_2F_7$ .

Fig. 4(b) shows how a slightly distorted version of  $R-Nb_2O_5$  is used to produce the crystal structure of  $\beta-U_3O_8$ <sup>32</sup> and the high-pressure modification of  $Nb_3O_7F$ <sup>33</sup>. These structures can also be derived from modules of the  $R-Nb_2O_5$  type involving *one* set of twin planes.<sup>7</sup>

Fig. 4(c) shows the crystal structure of  $UMo_2O_8$  derived from  $R-Nb_2O_5$ .<sup>34</sup>

### Local twin planes and the $ReO_3$ -type structure

In an earlier paper<sup>5</sup> we discussed the compatibility of PCs with the  $ReO_3$ -type structure and presented a symbolism to aid in the description of the structures concerned. Here we would like to make some further relevant remarks.

It appears that the inter-relation of PCs and the  $ReO_3$ -type structure is closely connected with a special kind of

twin operation. The situation is best described by some examples. Fig. 5(a) shows two PCs embedded in an  $ReO_3$ -type matrix as described earlier.<sup>5</sup> In Fig. 5(b) we show how a single fourling unit of the TTB type [Fig. 2(e)] in  $ReO_3$  is associated with the atomic arrangement. In this case the twin planes have a limited extension in space. We therefore consider them as *local* twin planes. A regular arrangement of isolated fourling units with C/PCs is found in  $W_{12}O_{34}$ <sup>35</sup> and in  $4Nb_2O_5-22WO_3$  and  $4Nb_2O_5-50WO_3$ .<sup>36</sup>

Other arrangements of local twin planes with PCs occur in so-called reorientation boundaries in  $WO_3$ -rich samples in the  $Nb_2O_5-WO_3$  system.<sup>37</sup> Fig. 5(c) shows an arrangement in a meander form and Fig. 5(d) in a saw-tooth form. An arrangement similar to the latter type can be found in a compound related to the TTB structure (see below). The overall composition for the structures shown in Figs. 5(a)–(d) is  $MO_{3-x}$  with  $x > 0$ . Fig. 5(e) shows other sets of local twin planes with pentagonal bipyramids in an environment of ordinary  $ReO_3$ . The arrangement of the twin planes is

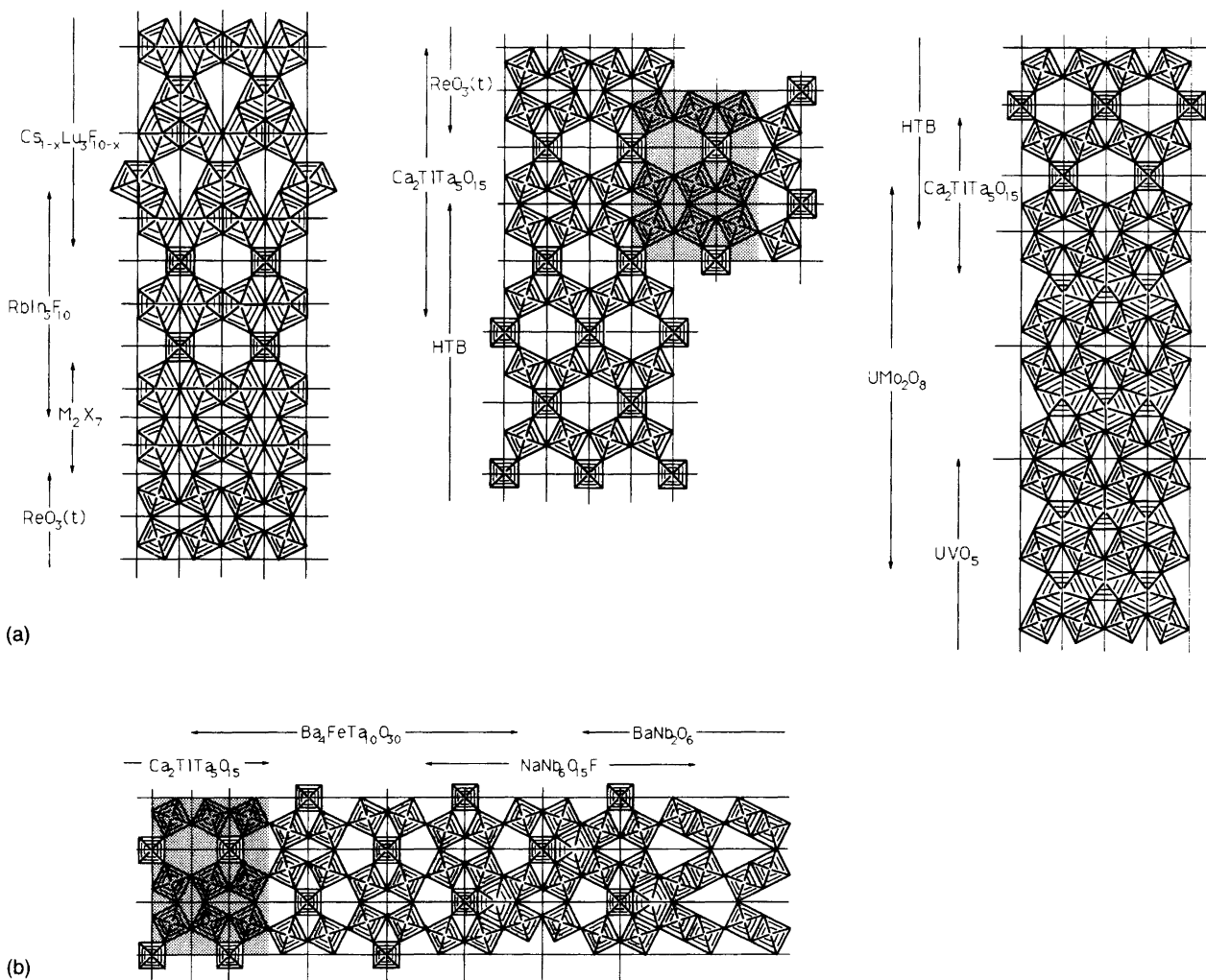


Fig. 6. A scheme of intergrowths centred on the structure of  $Ca_2TiTa_5O_{15}$ . Possible intergrowths along one direction are shown in (a) and in a perpendicular direction in (b). The same part of the structure of  $Ca_2TiTa_5O_{15}$  is shaded in (a) and (b). Note that only skeleton structures are shown; the large cations in the tunnels are not indicated.

similar to that in Figs. 5(b)–(d), but the overall composition differs and can be given as  $MX_{3+x}$  with  $x > 0$ . This fact may be of interest in case of non-stoichiometry in anion-excess  $ReO_3$  phases, e.g.  $Zr(F,O)_{3+x}$ ,  $x > 0$ .<sup>14,38,39</sup>

### Fourling structures and intergrowths

Several of the structures derived above should be able to intergrow with each other. In Figs. 6(a) and (b) we show this schematically, using our structural models. Among other things we may notice the following. First we observe that intergrown structures have a set of twin planes in common. Secondly we note that  $Ca_2TiTa_5O_{15}$  is able, according to this model, to form intergrowths with  $ReO_3(t)$  and HTB (ITB, see below) along one direction [Fig. 6(a)] and with  $Ba_4FeTa_{10}O_{30}$  (or  $NaNb_6O_{15}F$ ) along a perpendicular direction [Fig. 6(b)]. Thirdly,  $Ca_2TiTa_5O_{15}$  appears as an intermediate structure between HTB and  $ReO_3(t)$  or HTB and  $UMo_2O_8$  or  $UVO_5$ .

$M_2X_7$  and  $ReO_3$ . In addition to the atomic configurations of Fig. 5(e) resulting in an  $MX_{3+x}$  composition, we may obtain similar results from intergrowths between  $ReO_3(t)$  and orthorhombic  $M_2X_7$  [Fig. 6(a)]. Fig. 7(a) shows  $ReO_3(t)$  intergrown with a row of pentagonal bipyramids. Fig. 7(b) shows an arrangement derived through a cyclic reflection operation on part of the structure in Fig. 7(a). The unit at the centre of Fig. 7(b) is used as a fourling to derive the structure shown in Fig. 7(c) through twinning. It has the composition  $MX_{3.5}$ .

Intergrowth with ordinary  $ReO_3$  can be achieved by use of the hatched fourling unit in Fig. 1(c), as shown in Fig. 5(e). By modifying this fourling unit as shown in Fig. 8(a) we may obtain a structure composed of equal proportions of octahedra and pentagonal bipyramids [Fig. 8(b)]. This structure may also intergrow with ordinary  $ReO_3$  along sections indicated by arrows in the figure. A cyclic reflection of part of this structure is shown in Fig. 8(c).

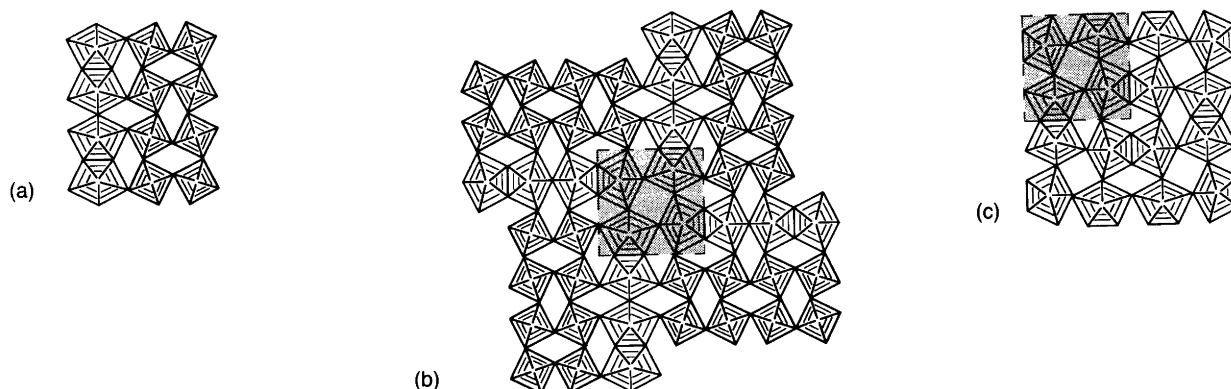


Fig. 7. (a) Possible intergrowth between orthorhombic  $M_2X_7$  and  $ReO_3(t)$ . (b) A fourfold operation on the structure in (a). (c) A structure derived by a fourling operation on the unit at the centre of (b).

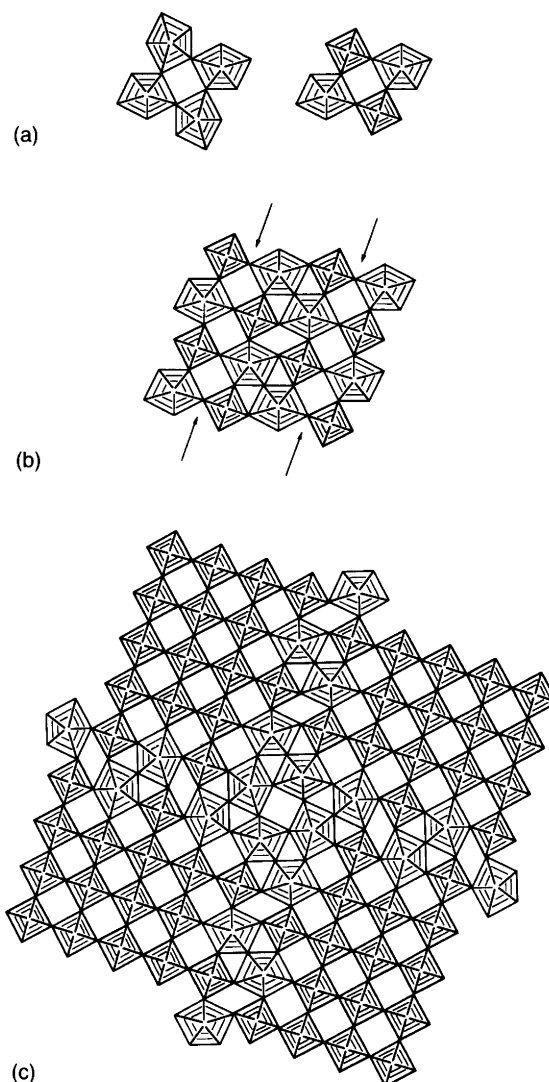
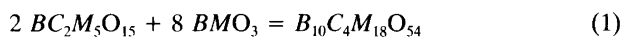


Fig. 8. (a) The unit from Fig. 1(c) modified to comprise two octahedra and two pentagonal bipyramids. (b) A structure built up from the modified unit in (a). Intergrowth with ordinary  $ReO_3$  is possible along the directions shown by arrows. (c) A fourfold rotation of part of the structure in (b), intergrown with ordinary  $ReO_3$ .

*TTB and perovskite.* Fig. 9(a) shows the crystal structure of  $\text{Ba}_{3.75}\text{Pr}_{9.75}\text{Ti}_{18}\text{O}_{54}$ .<sup>40</sup> The structure consists of ordered lamellae of TTB and perovskite. A TTB lamella embraces twin planes in a sawtooth arrangement. The width of a lamella is  $a_{\text{TTB}}/2$  and the stoichiometry is  $\text{BC}_2\text{M}_5\text{O}_{15}$ , where  $B$  and  $C$  stand for atoms with 12- and 15-coordination, respectively, in the TTB structure. The perovskite lamella shown in the figure comprises four unit cells ( $\text{BMO}_3$ ), and the structure will have the formula shown in eqn. (1). We



may of course vary the width of the perovskite lamella. Fig. 9(b) shows an example. The structure, so far not re-

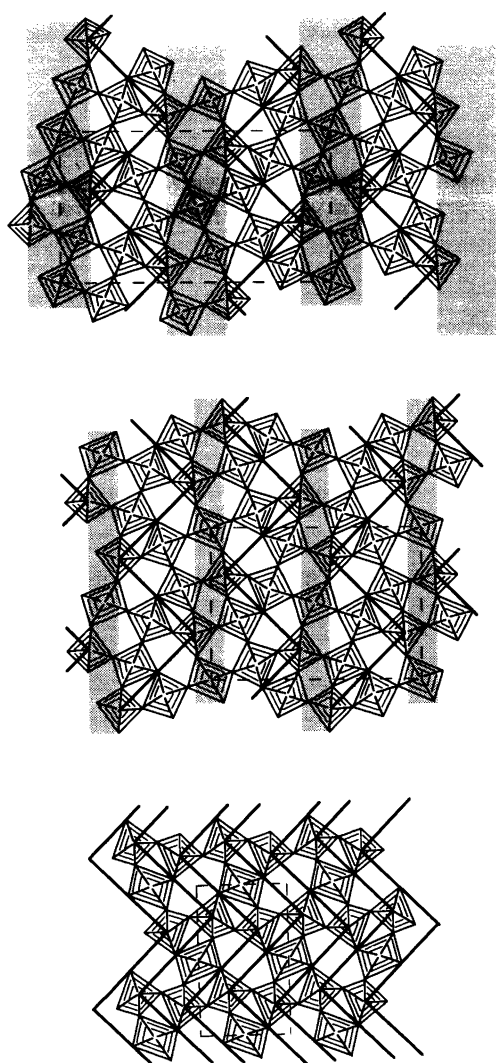
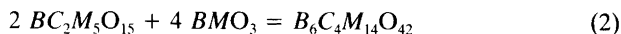


Fig. 9. (a) The crystal structure of  $\text{Ba}_{3.75}\text{Pr}_{9.75}\text{Ti}_{18}\text{O}_{54}$ .<sup>40</sup> Only the Ti-O network is shown. Local twin planes are shown in bold outline. The shaded area indicates a structure of the perovskite type. (b) The hypothetical structure of composition  $\text{B}_6\text{C}_4\text{M}_{14}\text{X}_{42}$ . (c) The crystal structure of deformed HTB [cf. Fig. 10(a)] obtained from areas contained between twin planes in TTB.

ported for any observed compound, has the theoretical composition of eqn. (2). In fact we may vary the number



of unit cells in the perovskite lamella from zero and upwards (zero, of course, gives the normal TTB structure). It is even possible to allow the TTB lamellae to overlap. Such a case is illustrated in Fig. 9(c). The result is in fact a distorted HTB structure. The width of the TTB lamella can also be varied, leading to other types of TTB-related structures. This has been discussed by Isupov,<sup>41</sup> who uses a different approach to the topic than the one applied here.

*HTB and  $\text{ReO}_3(t)$ .* The HTB structure [Fig. 10(a)] is adopted by some non-stoichiometric compounds.<sup>19</sup> For oxides the general formula is  $\text{A}_x\text{WO}_3$ , where  $A$  is an alkali or other electropositive metal atom. Some of the tungsten atoms may be replaced by lower-valent atoms of suitable size.<sup>42</sup> Oxide fluorides like  $\text{K}_x\text{NbO}_{2+x}\text{F}_{1-x}$ <sup>43</sup> and fluorides,  $\text{K}_x\text{FeF}_3$ ,<sup>44</sup> are also known with the HTB structure.

As is seen in Fig. 6(a), HTB may intergrow with the  $\text{ReO}_3(t)$  type via a structure of the  $\text{Ca}_2\text{TiTa}_5\text{O}_{15}$  type. Early examples of intergrowth tungsten bronzes (ITB) with partially reduced tungsten oxide ( $\text{A}_x\text{WO}_3$  with  $A = \text{K}, \text{Rb}, \text{Cs}, \text{Ti}$ ) have been reported by Hussain and Kihlberg,<sup>12</sup> who have also provided a nomenclature for the classification of ITB structures.

Examples of fully oxidized HTB phases intergrown with the  $\text{ReO}_3(t)$  type are  $\text{Ca}_2\text{MTa}_5\text{O}_{15}$  ( $M = \text{Tl}, \text{Rb}, \text{Cs}$ ),<sup>18</sup> and  $\text{ACu}_3\text{M}_7\text{O}_{21}$  ( $A = \text{K}, \text{Rb}, \text{Cs}, \text{Ti}; M = \text{Nb}, \text{Ta}$ )<sup>45</sup> [Figs. 10(b) and (c)]. Reviews of studies of tungsten bronzes and of fully oxidized, isostructural bronzoids have been given by Kihlberg<sup>46</sup> and by Sharma.<sup>42</sup>

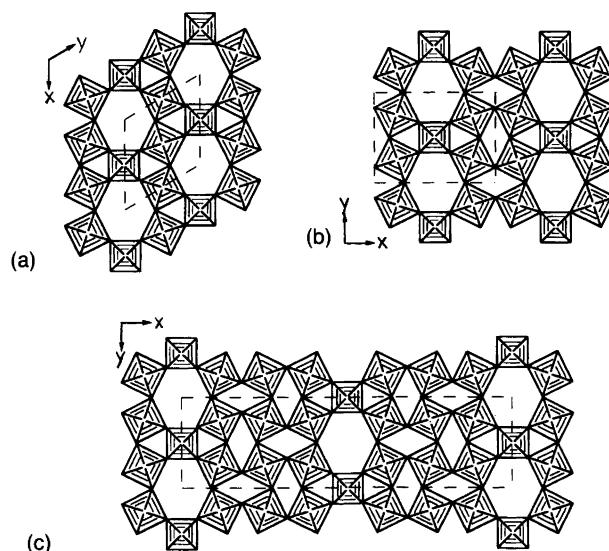


Fig. 10. The crystal structures of (a) HTB,<sup>19</sup> (b)  $\text{Ca}_2\text{MTa}_5\text{O}_{15}$  ( $M = \text{Tl}, \text{Rb}, \text{Cs}$ )<sup>18</sup> and (c)  $\text{ACu}_3\text{M}_7\text{O}_{21}$  ( $A = \text{K}, \text{Rb}, \text{Cs}, \text{Ti}; M = \text{Nb}, \text{Ta}$ ).<sup>45</sup> The structures in (b) and (c) are intergrowths of HTB and  $\text{ReO}_3(t)$ .



### Models of defects observed in HTB-related structures

Studies of HTB-related structures by high-resolution electron microscopy (HREM) have revealed the occurrence of disorder and of defects of various kinds. We intend to describe some observed defects in the light of the concepts of chemical twinning and local twin planes. Our starting point will be observations from samples of  $\text{Cs}_x\text{Nb}_x\text{W}_{1-x}\text{O}_3$ ,  $x = 0.1$ .<sup>42</sup> In these samples HTB-type slabs, three tunnel rows wide and wholly confined within a matrix of  $\text{WO}_3$ , were observed. The structure of the slab ends differs

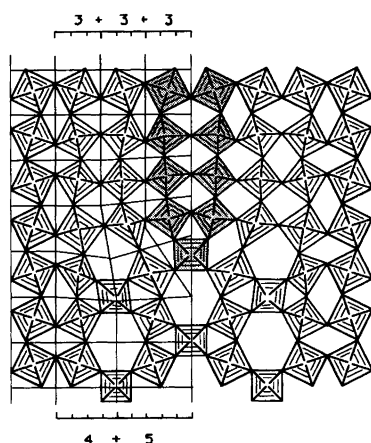


Fig. 11. Model of a triple row of six-sided tunnels in an  $\text{ReO}_3(\text{t})$  matrix. This triple terminates with five-sided tunnels at the outer rows. Fourling units with scales are indicated to the left in the figure. Note that the rows of shadowed octahedra in the  $\text{ReO}_3$  matrix terminate at the head of the triple row.

depending on the extensions of the central and outer rows. The structural details were interpreted from HREM images, and structural models were given.

We will use some of the fourling units derived above to show how their use may facilitate the description of the behaviour of tunnel rows in a matrix of the  $\text{ReO}_3(\text{t})$  type. We then rely on the interpretation given by Sharma.<sup>42</sup> Fig. 11 shows one of the models in which the outer rows are terminated by five-sided tunnels. We notice first that a twin plane at the centre of the triple row continues into the  $\text{ReO}_3(\text{t})$  part of the structure. Secondly, two rows of octahedra (shadowed) that emerge from the  $\text{ReO}_3(\text{t})$  part terminate at the head of the triple row. Thirdly, there is a certain distortion of the fourling units in the model. The disturbance caused by the termination of the triple row is, however, localized and can, according to this model, be made to fit exactly into the surrounding  $\text{ReO}_3(\text{t})$  structure.

We will conclude by showing a model of an HTB structure embedded in  $\text{ReO}_3(\text{t})$  and refer to the observations of strips of  $\text{WO}_3$ -type structure in three directions in an HTB-type crystal from a sample of  $\text{Cs}_x\text{Nb}_x\text{W}_{1-x}\text{O}_3$  with  $x = 0.12$ .<sup>47</sup> For this purpose we use the model of the triple-row defect shown in Fig. 11. Three triples are arranged side by side and stepwise as shown in Fig. 12(a). This configuration is then twinned along a plane perpendicular to the extension of the triples as illustrated in Fig. 12(b), which shows an HTB structure in a matrix of  $\text{ReO}_3(\text{t})$ .

### Conclusions

We have shown how fourling units derived from  $\text{ReO}_3$  or from structures related to  $\text{ReO}_3$  can be used to describe

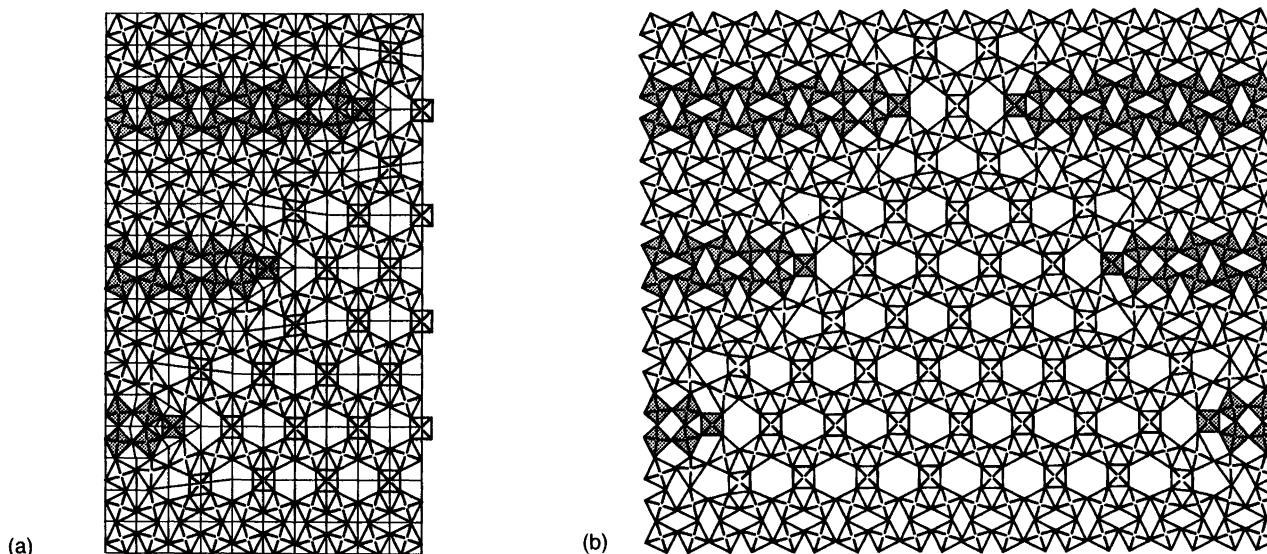


Fig. 12. (a) Triple rows of six-sided tunnels terminating in a matrix of  $\text{ReO}_3(\text{t})$  as shown in Fig. 11 are arranged stepwise side by side. Twinning of the arrangement in (a) along a plane perpendicular to the extension of the triple rows gives the configuration in (b), which shows an HTB structure completely embedded in  $\text{ReO}_3(\text{t})$ .

several complicated structures of oxides, fluorides and oxide halogenides. These structures can be classified into three main types according to their composition, namely  $A_yMX_3$  (I),  $A_yMX_{3-z}$  (II) and  $A_yMX_{3+z}$  (III).  $M$  and  $X$  are atoms constituting the network structure,  $0 < z \leq 0.5$ .  $A$  represents the cations inserted into the tunnels of the network structure,  $y \geq 0$ . Type I includes tungsten bronzes of the HTB and ITB types,  $Ca_2TiTa_5O_{15}$ ,  $Ba_4FeTa_{10}O_{30}$  and  $ReO_3(t)$ . Type II is represented by  $NaNb_6O_{15}F$ ,  $Nb_3O_7F(hp)$ ,  $\alpha-U_3O_8$  and  $UMo_2O_8$ . Type III, finally, is represented by  $KIn_2F_7$ ,  $U_2O_2Cl_5$ ,  $RbIn_3F_{10}$ ,  $Rb_2In_3F_{11}$  and  $Cs_{1-x}Lu_xF_{10-x}$ . Several of these structures can form intergrowths with each other.

We have also shown that there is a relationship between local twin planes and fourling units of tetragonal symmetry. The isolated fourling unit of the TTB type in an environment of the  $ReO_3$  type is an example. Local twin planes in the saw-tooth form are present in the TTB related structure of  $Ba_{3.75}Pr_{0.75}Ti_{18}O_{54}$ . They are formed as a consequence of the splitting of the fourling units when perovskite lamellae are introduced into the TTB structure. Local twin planes in the meander and saw-tooth form accommodating PCs are also observed in the  $Nb_2O_5-WO_3$  system. Finally it is shown that fourling units can conveniently be used in describing some defects observed in HREM studies of transition-metal oxides of the HTB and ITB types.

**Acknowledgements.** The author thanks Professor Lars Kihlberg and Dr. Margareta Sundberg for valuable discussions. This study has been supported by the Swedish Natural Science Research Council.

## References

- Andersson, S. and Hyde, B. G. *J. Solid State Chem.* 9 (1974) 92.
- Hyde, B. G., Bagshaw, A. N., Andersson, S. and O'Keeffe, M. *Annu. Rev. Mater. Sci.* 4 (1974) 43.
- Bovin, J.-O. and Andersson, S. *J. Solid State Chem.* 20 (1977) 127.
- Hyde, B. G. and Andersson, S. *Inorganic Crystal Structures*, Wiley, New York 1989, p. 95.
- Marinder, B.-O. *Angew. Chem., Int. Ed. Engl.* 25 (1986) 431.
- Lundberg, M. *Chem. Commun. Univ. Stockholm No. 7* (1971).
- Marinder, B.-O. *Acta Chem. Scand.* 44 (1990) 123.
- Hyde, B. G., Andersson, S., Bakker, M., Plug, C. M. and O'Keeffe, M. *Progr. Solid State Chem.* 12 (1980) 273.
- Van Landuyt, J., Amelinckx, S., Kohn, J. A. and Eckart, D. W. *J. Solid State Chem.* 9 (1974) 103.
- Bovin, J.-O. and Andersson, S. *J. Solid State Chem.* 18 (1976) 347.
- Glazer, A. M. *Acta Crystallogr., Sect. B* 28 (1972) 3384.
- Hussain, A. and Kihlberg, L. *Acta Crystallogr., Sect. A* 32 (1976) 551.
- O'Keeffe, M. and Hyde, B. G. *Acta Crystallogr., Sect. B* 33 (1977) 3802.
- Papiernik, R., Frit, B. and Gaudreau, B. *Rev. Chim. Miner.* 23 (1986) 400.
- O'Keeffe, M. and Hyde, B. G. *Philos. Trans. R. Soc. London, Ser. A* 295 (1980) 553.
- Scheffler, J. and Hoppe, R. *Z. Anorg. Allg. Chem.* 521 (1985) 79.
- Champarnaud-Mesjard, J. C., Mercurio, D. and Frit, B. *J. Inorg. Nucl. Chem.* 39 (1977) 947.
- Ganne, M., Dion, M., Verbaere, A. and Tournoux, M. *J. Solid State Chem.* 29 (1979) 9.
- Magnéli, A. *Acta Chem. Scand.* 7 (1953) 315.
- Brandt, R. and Müller-Buschbaum, Hk. *Z. Anorg. Allg. Chem.* 542 (1986) 18.
- Andersson, S. *Acta Chem. Scand.* 19 (1965) 2285.
- Marinder, B.-O., Wang, P.-L. and Werner, P.-E. *Acta Chem. Scand., Ser. A* 40 (1986) 467.
- Magnéli, A. *Arkiv. Kemi I* (1949) 213.
- Hyde, B. G. and O'Keeffe, M. *Acta Crystallogr., Sect. A* 29 (1973) 243.
- Champarnaud-Mesjard, J.-C. and Frit, B. *Acta Crystallogr., Sect. B* 34 (1978) 736.
- Sturm, J., Gruehn, R. and Allmann, R. *Naturwissenschaften* 62 (1975) 296.
- Metin, J., Chatonier, D., Avignant, D., Chevalier, R. and Cousseins, J. C. *J. Solid State Chem.* 55 (1984) 299.
- Marinder, B.-O. *Chem. Scr.* 26 (1986) 547.
- Gruehn, R. *J. Less-Common Met.* 11 (1966) 119.
- Levet, J. C., Potel, M. and Le Marouille, J. Y. *J. Solid State Chem.* 32 (1980) 297.
- Champarnaud-Mesjard, J.-C. and Frit, B. *Acta Crystallogr., Sect. B* 33 (1977) 3722.
- Loopstra, B. O. *Acta Crystallogr., Sect. B* 26 (1970) 656.
- Jahnberg, L. *Chem. Commun. Univ. Stockholm, No. 17* (1971).
- Cremers, T. L., Eller, P. G., Penneman, R. A. and Herrick, C. C. *Acta Crystallogr., Sect. C* 39 (1983) 1163.
- Sundberg, M. *Chem. Scr.* 14 (1978-79) 161.
- Iijima, S. *Acta Crystallogr., Sect. A* 34 (1978) 922.
- Iijima, S. and Allpress, J. G. *Acta Crystallogr., Sect. A* 30 (1974) 29.
- Tofield, B. C., Poulain, M. and Lucas, J. J. *J. Solid State Chem.* 27 (1979) 163.
- Poulain, M., Poulain, M. and Lucas, J. J. *J. Solid State Chem.* 8 (1973) 132.
- Matveeva, R. G., Varfolomeev, M. B. and Il'yushchenko, L. S. *Russ. J. Inorg. Chem.* 29 (1984) 17.
- Isupov, V. A. *Ferroelectrics* 76 (1987) 107.
- Sharma, R. *Chem. Commun. Univ. Stockholm, No. 3* (1985).
- de Pape, R., Gauthier, G. and Hagenmuller, P. *CR Seances Acad. Sci., Ser. C* 266 (1968) 803.
- de Pape, R. *CR Seances Acad. Sci., Ser. C* 260 (1965) 4527.
- Benmoussa, A., Groult, D., Studer, F. and Raveau, B. *J. Solid State Chem.* 41 (1982) 221.
- Kihlberg, L. In: Metselaar, R., Heijligers, H. J. M. and Schoonman, J., Eds., *Solid State Chemistry 1982, Proceedings of the Second European Conference 1982, Studies in Inorganic Chemistry, Vol. 3*, Elsevier, Amsterdam 1983, p. 143.
- Sharma, R. and Kihlberg, L. *Mater. Res. Bull.* 16 (1981) 377.

Received November 7, 1990.